



ORIGINAL ARTICLE

α -Linolenic acid alleviates aluminum toxicity in RAW264.7 cells by antioxidative and anti-inflammatory effects



Qiqi Ji ^{a,b}, Ling Han ^a, Tianyuan Zhang ^c, Xiaoyang Xia ^{a,*}, Xia Xiang ^{a,*}

^a Oil Crops Research Institute, Chinese Academy of Agricultural Sciences, Oil Crops and Lipids Process Technology National & Local Joint Engineering Laboratory, Key Laboratory of Oilseeds Processing, Ministry of Agriculture, Hubei Key Laboratory of Lipid Chemistry and Nutrition, Key Laboratory of Biology and Genetic Improvement of Oil Crops, Ministry of Agriculture, Wuhan 430062, China

^b Key Laboratory of Plant Resource Conservation and Germplasm Innovation in Mountainous Region (Ministry of Education), Collaborative Innovation Center for Mountain Ecology & Agro-Bioengineering (CICMEAB), College of Life Sciences/Institute of Agro-bioengineering, Guizhou University, Guiyang, Guizhou, China

^c State Key Laboratory of Agricultural Microbiology, College of Life Science and Technology, Huazhong Agricultural University, Wuhan, Hubei 430070, China

Received 17 July 2022; accepted 22 April 2023

Available online 26 April 2023

KEYWORDS

α -linolenic acid;
Inflammation;
Aluminum;
RAW264.7 cells;
RNA-seq

Abstract Aluminum is an inorganic contaminant and has adverse effects on human and animal health by mainly accumulating in the immune system to exert toxicity. α -Linolenic acid (ALA), a crucial dietary component, possesses various bioactivities. Nevertheless, the effects of ALA on Al-induced toxicity have not been sufficiently understood. In this study, we aimed to elucidate the possible mechanism of aluminium chloride hexahydrate ($AlCl_3 \cdot 6H_2O$, Al) exposure to RAW264.7 cells and the response of ALA through an RNA sequencing (RNA-seq). RNA-seq results demonstrated that Al exposure resulted in 2106 differentially expressed genes (DEGs) with 53 pathways, including the NF- κ B, enriched by the KEGG analysis. 200 of the 2106 DEGs were modulated in ALA-pretreated group, which were enriched into 36 pathways, containing the NF- κ B. qRT-PCR results displayed the RNA-seq's reproducibility and reliability. Western blot analysis confirmed that the protection of ALA against Al toxicity was associated with NF- κ B mediated JAK2/STAT3/SOCS3 pathway and HO-1 activation. These results elucidated the protection of ALA against Al-induced toxicity from a new perspective and provided a potential therapy for Al

* Corresponding authors.

E-mail addresses: xia_xiaoyang@126.com (X. Xia), xiangxia0130@163.com (X. Xiang).

Peer review under responsibility of King Saud University.



treatment.

© 2023 The Author(s). Published by Elsevier B.V. on behalf of King Saud University. This is an open access article under the CC BY-NC-ND license (<http://creativecommons.org/licenses/by-nc-nd/4.0/>).

1. Introduction

Aluminum is a widespread inorganic and environmental contaminant, presenting human health threats (Zhang et al., 2020a; Liu et al., 2022). The adverse effects of aluminum on health are aggravated due to the broad exposure in foods and sources in cosmetics, tea, drugs, and air, etc (Deng et al., 2011; Newairy et al., 2009). Previous study found that the Al toxicity was exerted mainly through accumulation in the immune system, leading to immune function suppression, considered as an immune toxic substance. Also, the overloading of aluminum in the organs of liver, blood and spleen leads to inflammatory response, further inducing severe damage to human health such as Parkinson, Alzheimer, liver dysfunction (Cheng et al., 2019). These will eventually pose heavy burdens associated with life and financial costs on family and society. Especially in the developing countries, the aluminum release from cookware was up to 125 mg/serving, which exceeded 6-fold of WHO's recommended intake (20 mg/day/person) (Weidenhamer et al., 2017). Aluminum contamination and inflammation are a growing public health risk. Exploring aluminum-induced immunotoxicity and revealing possible mechanisms deserve extensive attention.

Macrophages possess an essential function in modulating immune response employing pro-inflammatory and anti-inflammatory mechanisms. Mouse peritoneal macrophage RAW264.7 is a standard cell to study inflammation (Hu et al., 2011). Recent advances in immunotoxicity action of Al were reported. Hu's group demonstrated that drinking water with 52 mg/kg aluminum chloride (AlCl₃, Al) for 120 days in Wistar rats, phagocytosis capacity of peritoneal macrophages was greatly suppressed (Hu et al., 2011). 150 mg/kg Al exposure to intragastric administration in female Wistar rats with 90 days induced dysfunction of the peritoneal macrophages and increased the peritoneal inflammation (Ayuob, 2013). Bakour's group found that 662.2 mg/kg Al in rats induced toxicity by elevating C-reactive protein's inflammatory markers (Bakour et al., 2017). Oral administration of Al in rats with 90 days resulted in immunosuppression via Nrf2 signaling pathway (Yao et al., 2019). Wang's group uncovered that Al exerted toxicity in mouse RAW264.7 macrophages through MAPK/Akt signaling pathway (Cheng et al., 2019). Nevertheless, the mechanism of action of Al toxicity in macrophages is still poorly understood.

Recently, dietary compounds have attracted increasing concern due to the importance and low toxicity. As a omega-3 (Ω-3) polyunsaturated fatty acid needed for human health, α-linolenic acid (ALA) is known and important dietary component, which transfers to docosahexaenoic acid and eicosapentaenoic acid in vivo as a precursor molecule (Kim et al., 2014). Considerable evidence shows that ALA has essential pharmacological effects in treating various diseases, such as cardiovascular system, nervous disorders, colitis, etc (Ren and Chung, 2007). In our previous work, ALA attenuated Al toxicity in PC12 cells by mediating the PKA-CREB-BDNF signaling pathway (Liu et al., 2022). In addition, ALA possesses prominent anti-inflammatory activity (Gao et al., 2020). For example, ALA inhibited the production of inflammatory factor and inflammatory phenotype induced by lipopolysaccharide (LPS) (Gao et al., 2020). ALA administration dampened nitrite accumulation, prostaglandin E-2 production, and the expressions of COX-2 enzyme and iNOS (Jie et al., 2007). Moreover, low dosage ALA could remarkably ameliorate trinitrobenzene sulfonic acid (TNBS)-exerted colitis (Wen et al., 2019). It has been increasingly recognized the key role of ALA's anti-inflammation capacity in physical activity. However, the inflammation responses induced by metallic element is dissimilar from LPS and TNBS. Whether ALA has the potential action against aluminum-induced inflammation responses still needs to be clarified.

Transcriptome analysis is a high throughput technology to investigate gene expression profiles based on RNA-seq data, analyzing alternative splicing, and detecting posttranscriptional events with alteration of the external environment (Chen et al., 2020). RNA-seq has been widely employed to clarify the potential mechanisms of the event in food, medicine, environmental biology, and other fields (Zhang et al., 2020b). In contrast, it has rarely been performed to obtain information regarding the Al toxicity at the transcriptome level to date. Therefore, we herein used RNA-seq technology to identify the genes in RAW264.7 cells associated with inflammatory pathways that are involved in Al immunotoxicity and the protective effects of ALA. The critical signaling pathways were further verified using western blot analysis. This study aimed to extend the essential understanding of environmental pollution in Al toxicity and provided a potential of ALA to prevent Al-induced macrophage injury.

2. Materials & methods

2.1. Materials

ALA (purity ≥ 98%) was provided by Solarbio (Beijing, China). The stock solution of ALA in DMSO was kept at -20 °C for use. Dulbecco's modified Eagle's medium (DMEM) and fetal bovine serum (FBS) were obtained from Gibco (Life Technologies, Grand Island, NY). AlCl₃·6H₂O (Al, purity ≥ 97%) was brought from Sinopharm chemical (Shanghai, China). Al was dissolved in deionized water with a concentration of 4 M and stored at -20 °C for use. During the whole experiments, ALA and Al were diluted with culture medium without serum (DMEM). Malondialdehyde (MDA), reduced glutathione (GSH), and superoxide dismutase (SOD) assay kits, Annexin V-FITC/Propidium Iodide (PI) kit, protein extraction and quantitation kits were purchased from Nanjing Jiancheng Bioengineering Institute (Nanjing, China). The cell apoptosis dyes were gained from Keygen Biotech (Jiangsu, China). NO kit and ELISA kits (IL-6, IL-1β and TNF-α) were brought from Elabscience Biotechnology Co., Ltd (Wuhan, China).

2.2. Al exposure and ALA treatment

RAW264.7 cells were cultured in 1640 modified medium containing 10% fetal bovine serum (Gibco, USA) with 1% penicillin-streptomycin solution, and placed at cell incubator. The cells were cultured at 5% CO₂ and 37 °C. They were seeded in a 25 cm² culture flask (Falcon, Becton Dickinson) and were counted with a cell counter (Bio-Rad, USA) before seeding. Negative control, only medium without serum was added without Al. Al was prepared in a culture medium without serum at the concentrations of 2, 8, 10, 15 mM for 24 h. In the ALA treatment, cells were exposure to ALA prepared in a culture medium without serum alone for 24 h. For the ALA treatment experiment, RAW264.7 cells were co-incubated in ALA + Al mixture. Each condition (control, Al, ALA and the Al + ALA co-culture) with six independent replicates for further research.

2.3. Cell viability assay and oxidative stress activities

The RAW264.7 cells were cultured in 96-well plates for 24 h at a density of 5×10^4 cells per well. Different treatments (Control, Al and Al + ALA) were performed to RAW264.7 cells. After that, the 10 μ L Cell Counting Kit-8 (CCK-8) solution was added to each well for 30 min incubation. The most important chemical of CCK-8 kit is WST-8, named 2-(2-methoxy-4-nitrophenyl)-3-(4-nitrophenyl)-5-(2,4-disulfonic acid benzene)-2H-tetrazolium monosodium salt, which is reduced by dehydrogenases in cells to produce a yellow colored and soluble formazan dye in the tissue culture medium. Finally, the absorbance intensity of dye was recorded at 450 nm (SpectraMax M2, Molecular Devices, Sunnyvale, CA).

Intracellular ROS generation was assessed using a ROS assay kit (Beyotime, Shanghai, China) (Han et al., 2019). RAW264.7 cells with a density of 10^6 cell per well were seeded in 6-well plates. Following treatment with ALA and Al, cells were incubated with ROS probe (dichlorodihydrofluorescein diacetate, DCFH-DA) in the incubator for 30 min in the dark. Then cells were washed three times with PBS, and the fluorescence intensity of DCFH-DA of the stained cells was recorded with a micro-plate reader (excitation: 488 nm, emission: 525 nm).

Intracellular biochemical molecules like Malondialdehyde (MDA), reduced glutathione (GSH), and superoxide dismutase (SOD) play an important role in cell signaling against oxidative stress. The treated cells were harvested and sonicated at 4 °C. The supernatants were collected for the analysis of MDA, SOD, and GSH level by commercial kits following the manufacturer's instructions.

2.4. Cell apoptosis

The level of cell apoptosis was performed according to the instructions of 4',6-diamidino-2-phenylindole (DAPI) and Annexin V-FITC/Propidium Iodide (PI) staining assay kit. Briefly, the RAW264.7 cells were cultured in 6-well plates for 24 h at a density of 10^6 cells per well. After RAW264.7 cells treated for 24 h by 50 μ M of ALA with or without 10 mM of Al, the cells in 6-well plate were fixed with DAPI at 37°C for 15 min with three washing. The 6-well plate was washed with methanol and added with PBS. Morphological images after Al and ALA treatment were viewed with an inverted fluorescent microscope (Olympus IX71, Japan). On the other hand, the treatment HeLa cells were washed twice with PBS, resuspended with 500 μ L of binding buffer and then incubated with 5 μ L of Annexin V-FITC and 5 μ L of PI working solution for 10 min in dark. Stained cells was employed to quantify the cell apoptosis number combination with flow cytometry (BD Biosciences, USA).

2.5. Measurement of cytokines production

RAW264.7 cells were cultured in 12-well plates at a density of 5×10^5 cells per well overnight and then incubated with ALA for another 24 h with or without Al. After 24 h of culture, the cell supernatant was collected and centrifuged at 4 °C and 3000 r/min for 10 min. Release of NO in the culture supernatant was detected according to the manufacturer's instructions. TNF- α , IL-1 β , and IL-6 levels in the cell culture supernatant were

determined according to the ELISA kit instructions. All samples were measured in three independent replicates.

2.6. RNA sequencing and bioinformatics analysis

TRIzol reagent (Thermo Fisher, China) was extracted the total RNA separately from RAW264.7 cells and adopted for library preparation and sequenced (Illumina Inc., San Diego, CA, USA). Meanwhile, the RNA ratio of 28S/18S was up to 1.8 in each sample. First, SOAPnuke is used to conduct quality testing on the original data to obtain clean data of high quality (Chen et al., 2018). Then submitting to NCBI SRA database. And mapped to the mmu10 genome (Mus_GRCm38) using STAR v 2.7.0e with default parameters (Dobin et al., 2012). The gene expression level normalized as FPKM was analyzed with HTSEQ 0.10.0 package. The DEGs were identified by using DESeq2 packages as described the standard: $|\text{Fold change}| \geq 2$ $\text{FDR} < 0.05$ based on the three biological replicates (Love et al., 2014). Gene enrichment analysis were analyzed using ClusterProfiler package against GO and KEGG term. The PPI network prediction was carried out by mean of the STRING database (<https://string-db.org/>). The topological structure of PPI network was analyzed by Cytoscape (version 3.6.0) after obtaining the PPI pairs.

2.7. qRT-PCR and western blot analysis

The reverse transcription into cDNA was carried out by gDNA digester plus kit (yesen, Shanghai, China). The housekeeping gene GADPH was an internal reference. Primers for the 9 DEGs and GADPH (Table S1) were designed by Sangon Biotech (Shanghai, China). Then, qRT-PCR was performed with Hieff® qPCR SYBR® Green Master Mix (Yeasten, Shanghai, China) on a BioRad CFX96 system. The altered mRNA levels were determined employing the $2^{-\Delta\Delta Ct}$ method. Each sample was in three biological replicates.

RAW 264.7 cell line with different treatments was incubated on 6-well plates at a density of 10^6 cells per well with a certain density overnight. Collected cells were lysed with ice-cold RIPA lysis buffer and the protein concentration was detected with the BCA quantitative protein Kit. Subsequently, SDS-PAGE protein gels were used to separate those proteins, which was shifted to the PVDF membrane and blocked with PBST containing 5% skimmed milk (Millipore, Billerica, MA, USA) for 1 h. The PVDF membrane was treated separately with different primary antibodies overnight at 4 °C including p-p38 (1:1000, Cell Signaling, USA), JNK (1:1000, Cell Signaling, USA), ERK1/2 and p-ERK1/2 (1:1000, 1:2000, Cell Signaling, USA), COX-2 (1:1000, Cell Signaling, USA), SOCS3 (1:1000, Cell Signaling, USA), STAT3 (1:1000, Cell Signaling, USA), JAK2 (1:1000, Cell Signaling, USA), p-JAK2 (1:1000, Cell Signaling, USA), HO-1 (1:1000, Cell Signaling, USA), NF- κ B p65 (1:1000, Cell Signaling, USA), p-NF- κ B p65 (1:1000, Cell Signaling, USA), p38 (1:500–2000, Proteintech, China), Nrf2 (1:500–1000, ABclonal, China), iNOS (1:500–1000, ABclonal, China), p-JNK (1:1000–5000, ABclonal, China), p-STAT3 (1:500–2000, ABclonal, China), β -actin (1:5000–50000, Proteintech, China). Then, the secondary antibodies incubated. The blots were developed using chemiluminescent reagents (Immobilon™ western, Millipore, India) and scanned by Molecular Imager® Chemi-Doc™ XRS + with Image LAB™ Software.

2.8. Statistical analysis

All data was expressed as mean \pm S.D. Differences in various treatment groups were shown following Tukey's multiple comparison of one-way ANOVA. $P < 0.05$ represented statistical significance, $P < 0.01$ indicates extremely significance.

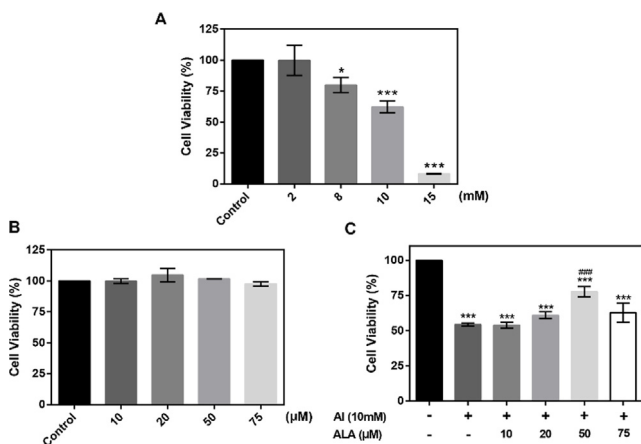


Fig. 1 The cytotoxicity of Al and ALA on RAW264.7 macrophages. (A) Al cytotoxicity. Cells were incubated with various Al concentrations (2–15 mM) for 24 h. (B) ALA cytotoxicity. Different amount of ALA was incubated with cells for 24 h. (C) Cell viability of ALA + Al co-culture. The data obtained from six individual experiments were collected shown as mean \pm SD. * $P < 0.05$, *** $P < 0.001$ vs. control group. # $P < 0.05$, ### $P < 0.001$ vs. Al group.

3. Results

3.1. The cytotoxicity of Al in RAW264.7 cells and the protective effects of ALA

RAW264.7 macrophages were treated with Al for 24 h. As shown in Fig. 1A, a dose-dependent decline of cell viability was observed with Al exposure from 2 to 15 mM compared to the control group. With the amount of Al up to 10 mM, cell survival reduced nearly 40% ($P < 0.001$), chosen for the subsequent studies. Meanwhile, different ALA concentrations from 10 to 75 μ M did not exhibit cytotoxicity (Fig. 1B). But a tendency toward higher cell survival with the increased concentration of the added ALA from 10 to 50 μ M in Al exposure (Fig. 1C). The cell viability increased by 23.4% in 50 μ M ALA treatment ($P < 0.001$) compared to Al exposure alone. While, the cell viability did not continually increase in Al treatment group when the concentration of ALA increased to 75 μ M. Therefore, 50 μ M ALA treatment was chosen in the following experiments.

3.2. Biochemical index detection

The intracellular ROS accumulation and relative enzyme activities in RAW264.7 cells were measured. Compared to the control group, Al exposure caused a more than two-fold enhancement of the intracellular ROS content (Fig. 2A, $P < 0.001$) and promoted a higher MDA level (Fig. 2B $P < 0.001$). ALA treatment markedly lowered the above actions ($P < 0.001$, $P < 0.01$). GSH and SOD levels were greatly reduced in the Al group (Fig. 2C and D, $P < 0.001$), which were recovered substantially after ALA treatment

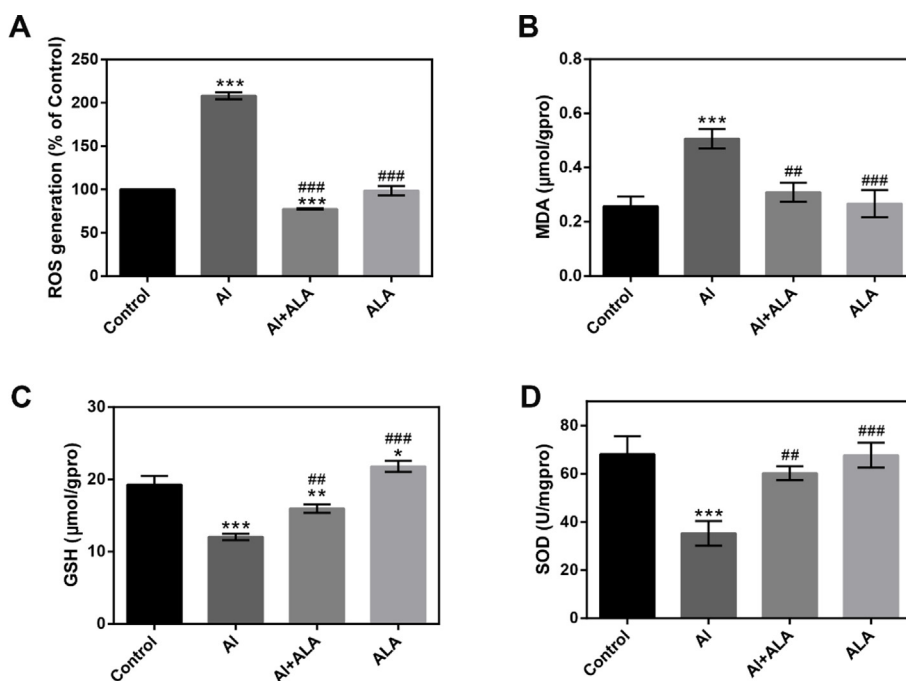


Fig. 2 Biochemical index analysis. Effects of Al and ALA on oxidative stress. (A) ROS level. (B) MDA activity, (C) GSH level and (D) SOD activity. The data obtained from three individual experiments were collected shown as mean \pm SD. * $P < 0.05$, ** $P < 0.01$, *** $P < 0.001$ compared with the control group. # $P < 0.05$, ## $P < 0.01$, ### $P < 0.001$ compared with Al group.

($P < 0.01$). ALA elevated the antioxidant capacity of cells to attenuate the immunotoxicity of Al.

3.3. Cell apoptosis

The influence of Al and ALA on cell apoptosis was evaluated using DAPI staining and flow cytometry (Fig. S1). Al exposure induced nuclear fragmentation and declined cell number, whereas they were converted in ALA treatment. The quantitative data displayed that Al treatment accelerated RAW264.7 cell apoptosis ratio by 20.17% ($P < 0.001$). In contrast, Al

and ALA co-treatment exhibited a lower apoptosis ratio of 22.7% ($P < 0.001$).

3.4. The expression of inflammatory cytokines and mediators

The release of pro-inflammatory cytokines was examined. Fig. 3A-C displayed that Al-induced severe inflammatory responses and significant enhancements in TNF- α , IL-1 β , and IL-6 production contrast to the control groups. In return, cells treated with ALA showed 65.0% decrease in the TNF- α

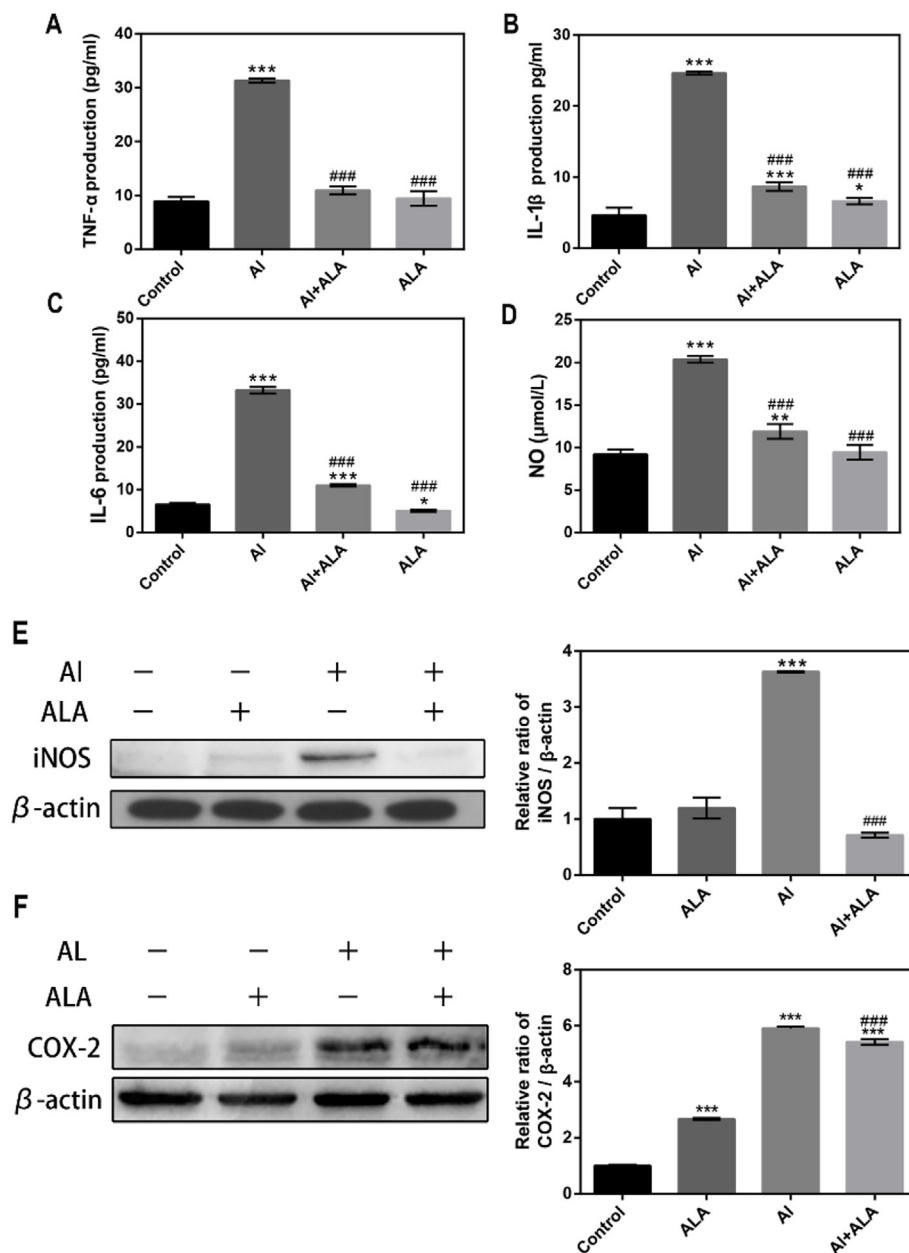


Fig. 3 The effects of Al and ALA on inflammatory cytokines and mediators in RAW 264.7 cells. (A) TNF- α level. (B) IL-1 β level. (C) IL-6 level. (D) NO content. (E) iNOS expression. (F) COX-2 expression. Various treatment conditions (control, Al, ALA, Al + ALA) were exposure to cells with 24 h incubation. The concentrations of Al and ALA were 10 mM and 50 μ M, respectively. Data obtained from three individual experiments was displayed as mean \pm SD. * $P < 0.05$, ** $P < 0.01$ and *** $P < 0.001$ vs. control group. # $P < 0.05$, ### $P < 0.001$ vs. Al group.

ing. 25.88 Gb of valid data from 516 million clean reads were gained after an effective filter. RNA-seq results exhibited that the Q30 of the raw reads was up to 93.28% in all samples (Table S2). The clean reads of 39,980,940–50,427,948 were gathered for each sample after effective filter (Q30 > 93.33%) (Supplementary Table 3).

3.6. DEGs analysis

We identify the DEGs according to the criteria: |fold-change| ≥ 2 and P-adjust < 0.05. Principal component analysis (PCA) was performed using fragments per kilobase of exon per million fragments mapped (FPKM) values to identify the sample clusters and distribution pattern (Li, et al., 2021). We used PCA to generate a genome-wide overview of the similarities and differences between control and Al-induced group and ALA + Al group. PCA displayed distinguished patterns among different treatment groups and similar expression patterns shared in each sample (Fig. 4A). Samples from control group fell on the positive side of X-axis while samples from

Al and Al + ALA groups fell on the negative side of X-axis. PCA analysis further showed that major portion of total variation (86.3%) consists of two principal components (PC1: 60.3%, PC2: 26.0%). The closer distance among spots exhibited more similarities in the principal components of samples. Nine pieces of the control (blue dots), Al (red dots), and ALA-treated (green dots) groups were clustered separately, showing the differentiation of gene expression patterns in different treatment groups and the excellent reproducibility in a single treatment condition. Compared to the control group, Al exposure identified 2106 DEGs containing 1119 up-regulated genes and 987 down-regulated genes (Fig. 4B). ALA treatment in the present of Al found 811 differentially expressed genes including 412 up-regulated genes, and down-regulated 399 genes (Fig. 4C). Notably, 388 DEGs was co-expressed both in Al and Al + ALA groups (Fig. 4D).

PPI analysis allows to directly or indirectly link proteins. Results showed PPI network prediction in different treatment groups. 50 most closely connected protein nodes were gained between the control group and Al exposure. 40 most closely

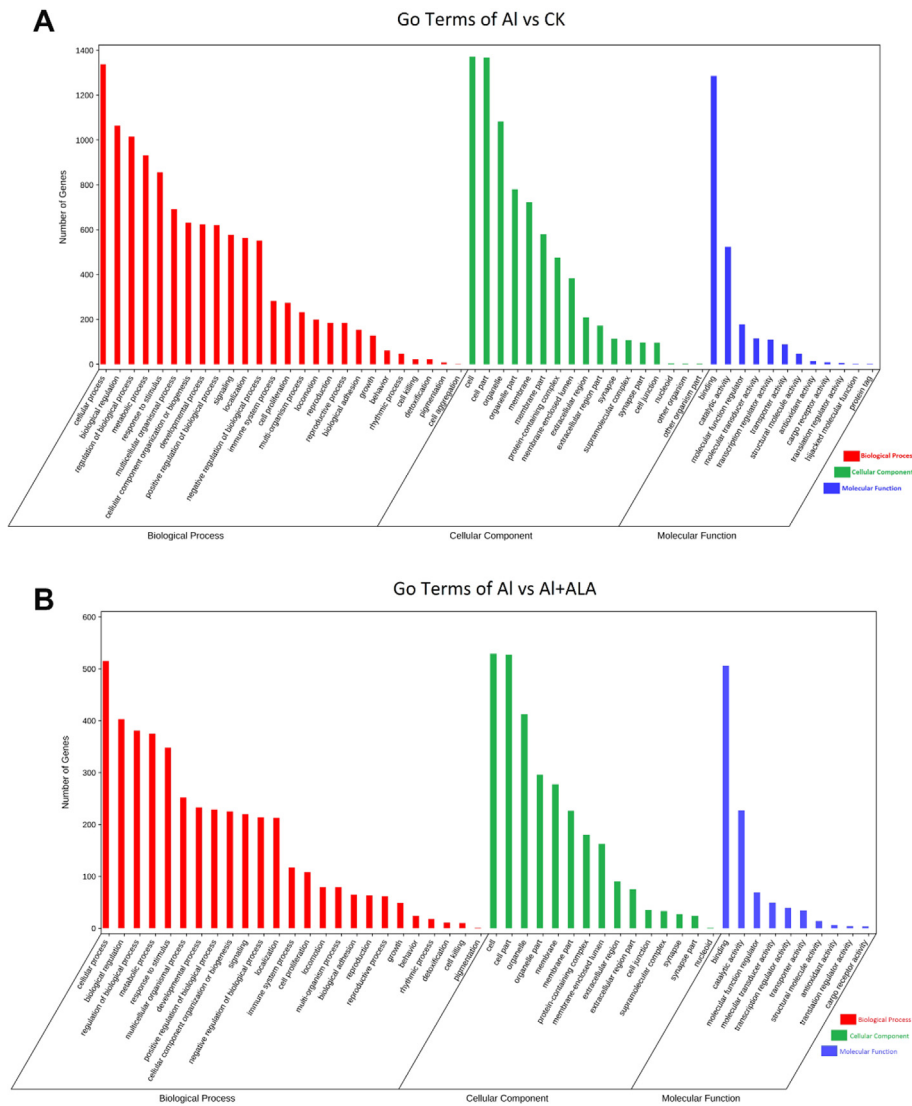


Fig. 5 GO functional classification analysis of DEGs. (A-B) GO term between the control vs Al group, and between the Al vs Al + ALA group.

related nodes were found between the AI group and ALA group (Fig. 4E-F).

In general, GO enrichment includes three groups: biological process; cellular components; molecular functions. In this system, GO annotations identified 282 DEGs in the AI group. The number of genes changed to 117 after ALA treatment (Fig. 5). Apparently, the most varied terms both in AI and ALA groups were enriched on binding of biological process, cellular components, and cellular processes of molecular functions. Notably, the alterations of response to stimuli, signaling, and immune system processes were simultaneously enriched in biological processes, which were closely associated with the immune system.

KEGG pathway was employed to analyze the obtained DEGs, and the results were present in Table S4 and S5. The 2106 DEGs identified in AI exposure were mainly enriched into 53 pathways. 811 DEGs were enriched into 36 pathways found with ALA treatment. Interestingly, the TNF, NF- κ B, and JAK/STAT pathways associated with the immune system were enriched in both groups. Meanwhile, the MAPKs pathway was markedly changed after AI exposure. The heatmap analysis exhibited that the AI group's enriched pathways contained inflammatory factors, chemokines, and upstream genes (Fig. 6). ALA treatment group had similar results.

3.7. Validation of expression using qRT-PCR

Random 9 genes from the DEGs were chosen (Cd40, Cxcl2, TnF, Birc3, Osm, Myc, Nfkbia, Tnfaip3, and Traf1) for qRT-PCR verification to confirm the RNA-seq's results. Significant upregulation was found in the AI group, while the expression was remarkably suppressed by ALA treatment. The qRT-PCR results described excellent consistency with the sequencing results, illustrating RNA-Seq's reproducibility and reliability (Fig. 7).

3.8. Western blot analysis

We examined protein expressions of the enriched pathways by western blotting analysis (Fig. 8). As MAPKs and NF- κ B pathway is one of the classical pathways in inflammatory apoptosis, the roles of the MAPKs pathway, and the expression of its related proteins were assessed. As shown in Fig. 7A and B, The expressions of phosphorylated proteins of p38, ERK1/2, JNK, and p65, significantly increased (3.1, 4.4, 1.6, and 1.6-fold, $P < 0.001$) following AI treatment. ALA treatment remarkably repressed these over-expressed proteins (46.7%, 8.3%, 19.7%, and 38.5% at the protein level, $P < 0.01$). These data indicated that ALA inhibited the impacts of AI toxicity by MAPKs and NF- κ B signaling pathways.

According to the essential role in inflammatory response regulation of JAK/STAT/SOCS3 pathway, we further explored whether JAK2/STAT3/SOCS3 pathway participated in AI toxicity and the protection of ALA. ALA suppressed AI-induced phosphorylation of JAK2 and STAT3 (82.5% and 18.8%, $P < 0.01$) with increasing SOCS3 expression (24.0%, $P < 0.001$).

Nrf2 can directly influence NF- κ B, including macrophages. HO-1 is an inducible enzyme exerting anti-inflammatory effects with overexpressed by translocating Nrf2 into the

nucleus. We further determined the expressions of HO-1 and Nrf2. ALA promoted Nrf2 protein expression and HO-1 activation (Fig. 9A). Interestingly, the Nrf2 protein expression was

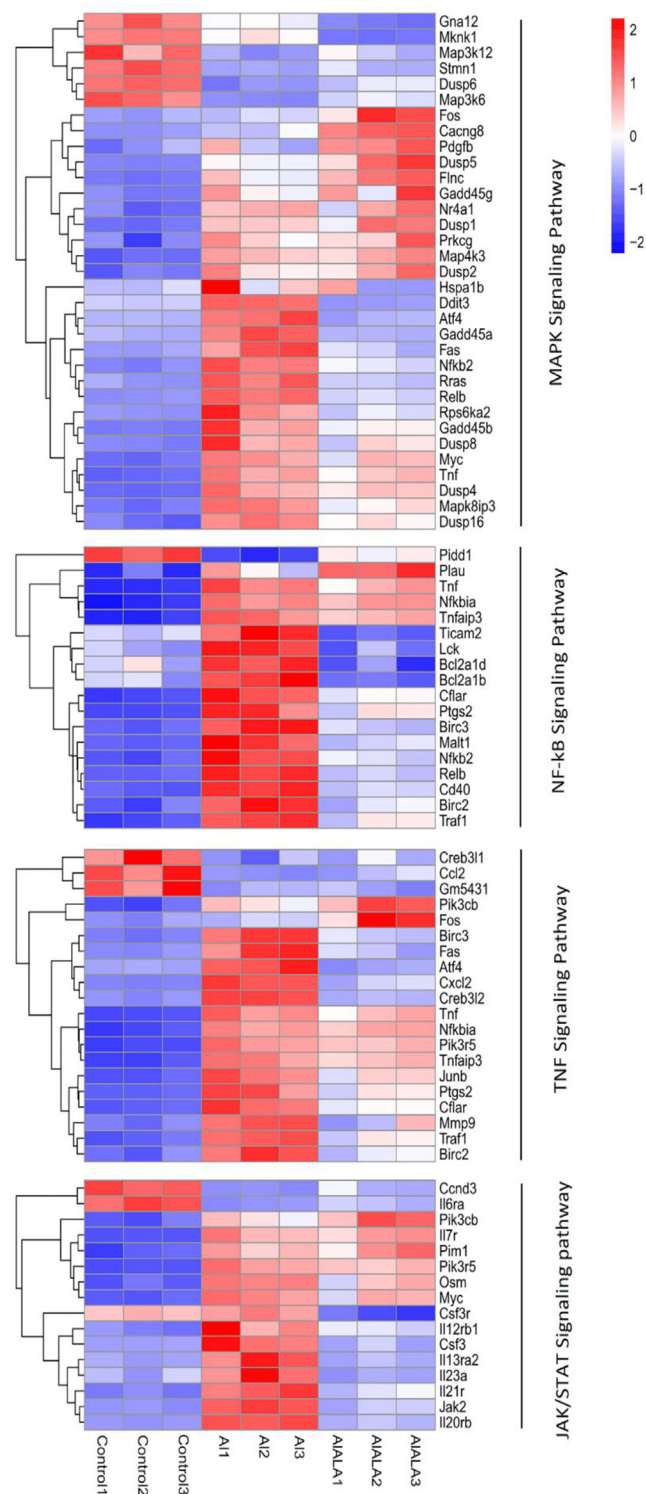


Fig. 6 KEGG classification of DEGs was performed based on FPKM data. Heatmap showed the mechanism of AI-induced inflammatory response AI and ALA's protection. Red represents up-regulated genes, and blue represent down-regulated genes. White represents an unchanged expression.

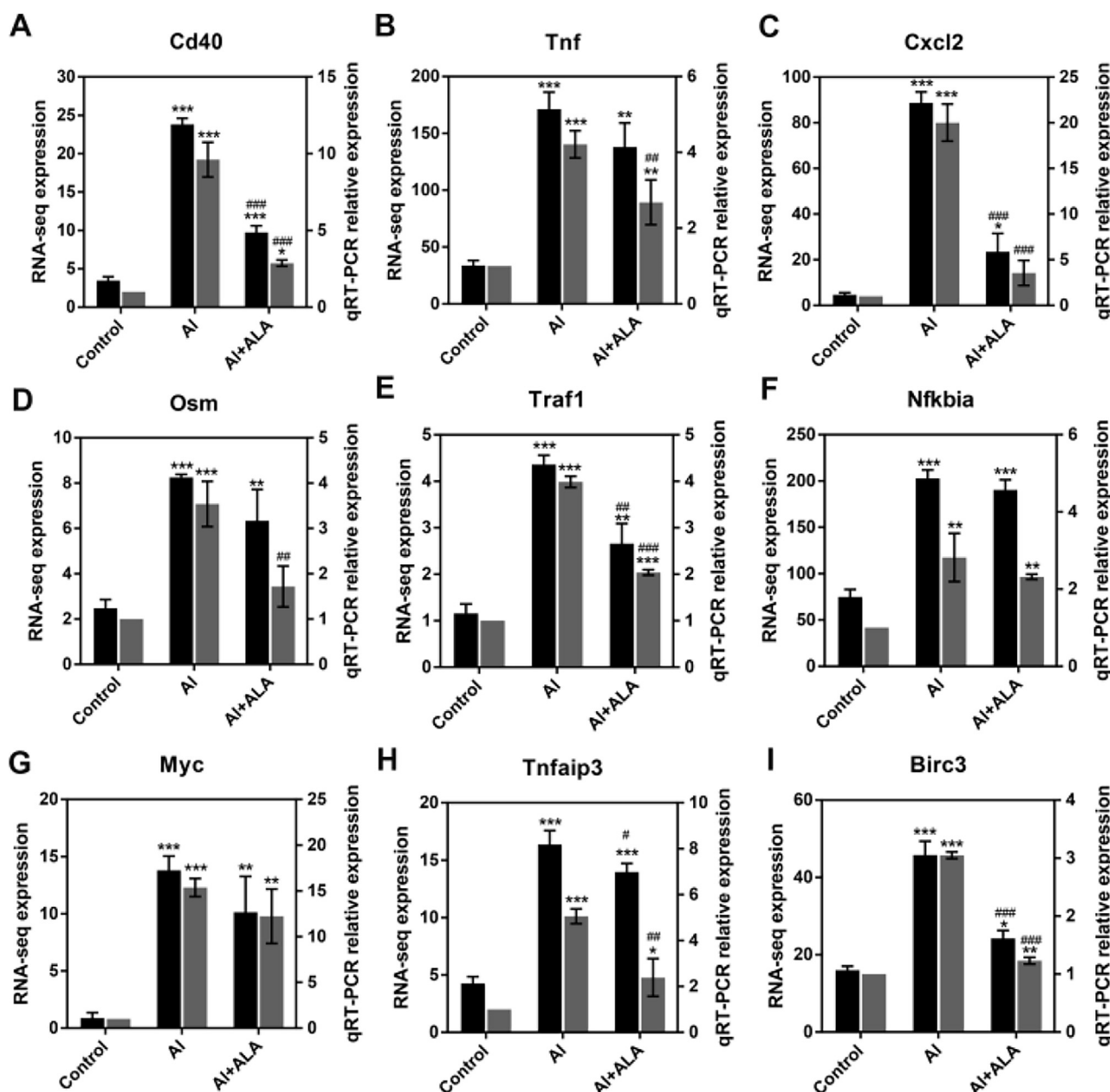


Fig. 7 qRT-PCR analysis for the validation of RNA-seq data. Random 9 DEGs (Cd40, Tnf, Cxcl2, Osm, Traf1, Nfkbia, Myc, Tnfaip3, Birc3) were selected. Data obtained from three individual experiments was displayed as mean \pm SD. **P < 0.01, ***P < 0.001 vs. control group. ##P < 0.01, ####P < 0.001 vs. Al group.

slightly reduced by ALA in Al exposure to RAW264.7 cells. Moreover, CoPP, a specific HO-1 inducer, hindering the generation of TNF- α and IL-6 after Al exposure (Fig. 9B). The Nrf2 pathway and HO-1 enzyme exerted a vital role in the Al toxicity toward RAW264.7 cells and in the suppressive response of ALA.

4. Discussion

Inflammation is a typical pathological process considered a stress response produced after being stimulated (Liu et al., 2019; Liu et al., 2022). An appropriate inflammatory response is benefit to remove pathogenic inflammatory factors, which is a protective effect for the body (Han et al., 2008; Hofseth and

Ying, 2006). Still, the excessive inflammatory response induces some diseases, including cancer, cardiovascular, neurodegenerative, and metabolism-related diseases (Abulfadl et al., 2018; Ye et al., 2019). Previous studies have shown that Al can cause inflammation and environmental pollutant (Zhang et al., 2018). As an essential polyunsaturated fatty acid (PUFAs), ALA has prominent anti-inflammatory activity (Gao et al., 2020). To our knowledge, RNA-seq analysis is first reported to evaluate the Al-induced toxicity against immune function and the protective potential of ALA against Al-induced toxicity.

ROS is mainly a product of oxidative metabolism in a biological organism, and a high ROS level causes direct damage (Farooq et al., 2019). MDA is a cytotoxic end product of lipid

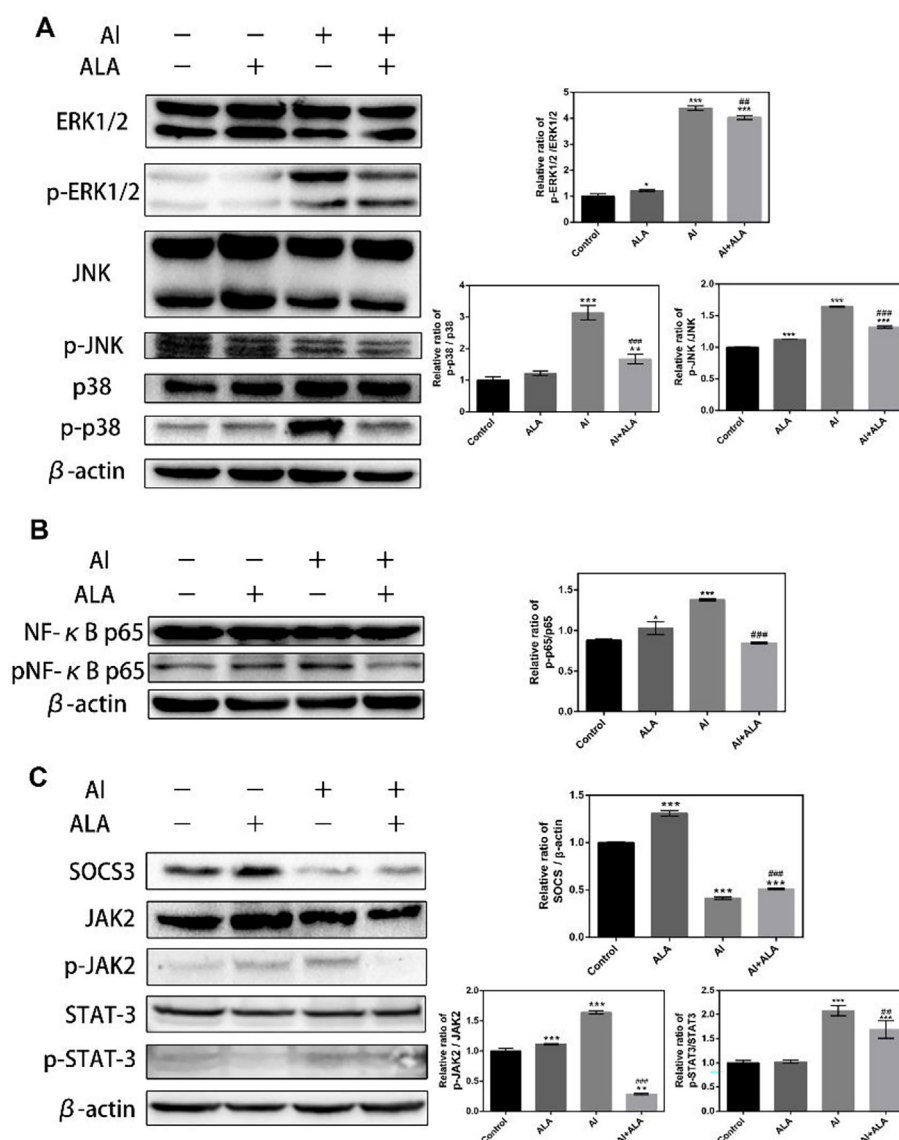


Fig. 8 The effects of Al and ALA on the enriched pathways using western blot analysis. (A-B) Effects of Al and ALA on NF-κB and MAPKs inflammatory signaling pathways by. (C) Effects of Al and ALA on the JAK2/STAT3/SOCS3 inflammatory signaling pathway. RAW264.7 macrophages were stimulated with Al (10 mM) alone or co-cultured with ALA (50 μM) for 24 h. Data obtained from three individual experiments was displayed as mean ± SD. **P < 0.01, ***P < 0.001 vs. control group. ###P < 0.01, ####P < 0.001 vs. Al group.

peroxidation due to polymerization with biological macromolecules, such as proteins and nucleic acid (Dimitrios and Tsikas, 2017). In this study, Al increased ROS and MDA content. In contrast, they decreased in the ALA group, suggesting that ALA can regulate oxidative stress levels in Al exposure to RAW264.7 (Fig. 2A-B). SOD and GSH are essential antioxidant enzymes in an organism and can remove harmful metabolic products. We found that Al significantly reduced SOD and GSH levels. However, they increased dramatically in the ALA group (Fig. 2C-D). Similar findings have been obtained in primary hippocampal neuronal cells and PC12 cells, and SH-SY5Y cells (Wang et al., 2018; Wang X, 2017). These results demonstrated that Al induced redox imbalance in RAW264.7 cells, but ALA ameliorated Al-induced toxicity associated with the antioxidant capacity of ALA.

It is well-recognized that the persistence of inflammatory cytokines may result in diseases caused by chronic inflammation. The previous study showed that the pro-inflammatory cytokines could induce inflammation by activating cellular signaling pathways involving MAPKs and NF-κB, which subsequently regulated gene expression of inflammatory cytokines through transcriptional and posttranscriptional mechanisms (Dong et al., 2020). Hence, the inhibition of inflammatory cytokines is crucial for alleviating inflammation. In this study, the overproduction of pro-inflammatory cytokines was obtained in Al treatment. ALA group inhibited pro-inflammatory cytokine production (Fig. 3A-C). iNOS and COX-2 participate in NO production, which is widely considered inflammatory mediators and regulated by NF-κB (Chou et al., 2019). Our results showed that Al treatment increased

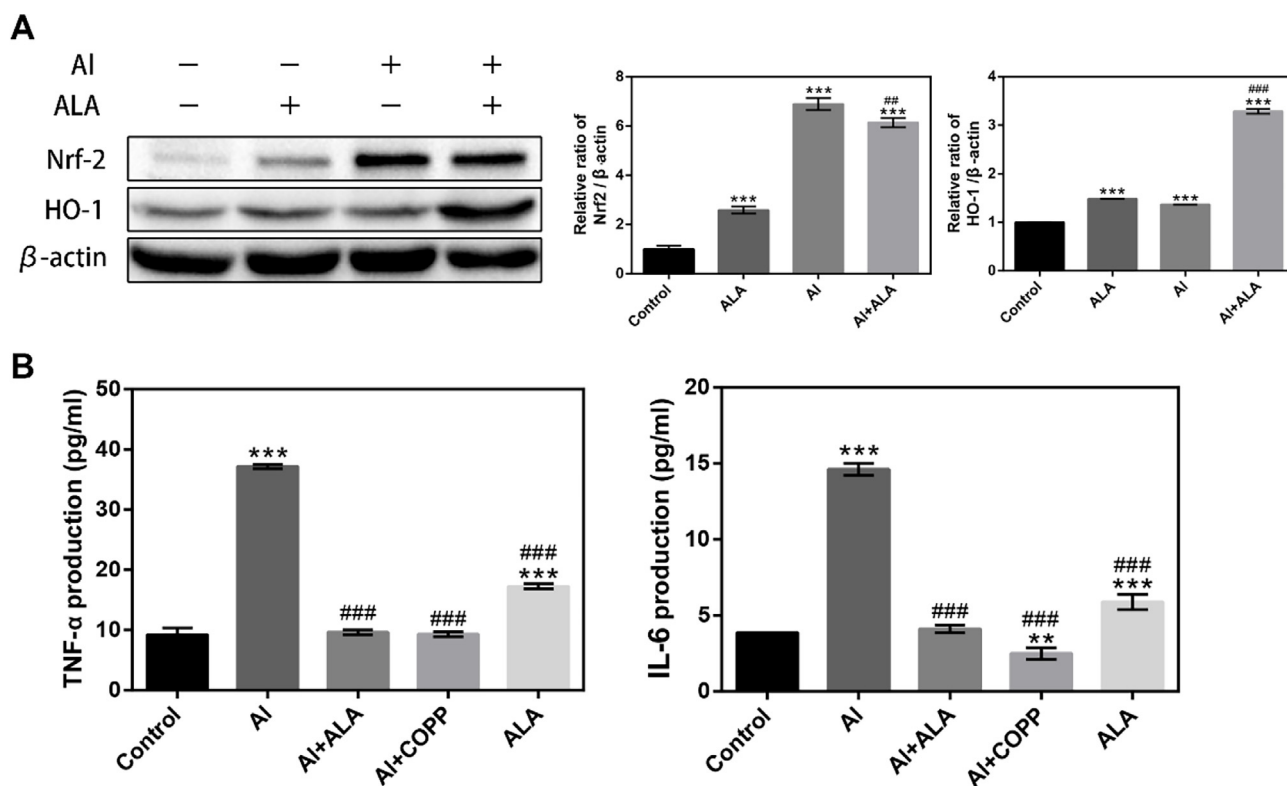


Fig. 9 ALA in Al-induced RAW264.7 cell can turn on the Nrf2 signaling pathway. (A) Western blot analysis of ALA on Nrf2/HO-1 inflammatory signaling pathways in Al-induced RAW264.7 cells. (B) HO-1 mediated the inhibitory effects of ALA on TNF- α and IL-6 in Al-induced RAW264.7 cells. The data obtained from three individual experiments were collected shown as mean \pm SD. **P < 0.01, ***P < 0.001 compared with the control group. ###P < 0.01, ###P < 0.001 compared with the Al group.

the expressions of iNOS, COX-2 expression, and NO, while the treatment of ALA significantly suppressed Al-induced enhancement of these expressions in RAW264.7 (Fig. 3D-F). ALA did not substantially inhibit cell viability in the absence and presence of Al (Fig. 1), confirming that there was no connection between the cytotoxic action of ALA and the inhibition of the production of NO and inflammatory cytokines. Similar mechanisms existed in grape leaves polyphenols-attenuated Al-induced toxicity (Borai et al., 2017). Al-induced inflammatory responses could be improved by ALA.

Despite Al generates prominent toxicities in the organism, the mechanism remains poorly known. According to the DEGs analysis identified by RNA-seq, Al exposure caused apparent alteration in the gene expression profiles (Fig. 4). ALA treatment induced significantly differential gene expression in contrast to Al exposure, indicating that the transcriptional pattern successfully distinguished the samples from ALA treatment with the Al group alone. GO terms from the specific genes suggested that the inflammation injuries are the primary target involved in Al-associated cellular toxicity and inhibition effects of ALA. The Al responsive genes (282 genes) were predominantly involved in the immune system, but the genes decreased to 117 after ALA treatment (Fig. 5A and B). According to the KEGG pathway enrichment results, TNF, NF- κ B, JAK/STAT, and MAPKs signaling might be the central pathway response to Al and ALA (Fig. 6). Correspondingly, we observed a prominent elevation of TNF- α and strong activation of NF- κ B p-p65 in the Al group transferred from cytoplasm to nucleus for promoting iNOS and COX-2 release

(Fig. 3E-F). As the reported study, Weng et al. showed that Al promoted TNF- α and IL6 production with NF- κ B p65 pathway activation (Weng et al., 2020). ALA treatment converted the changes, implying that NF- κ B has a crucial association with Al-induced toxicity.

The JAK-STATs cascade has been reported as a crucial inflammatory signaling pathway that could mediate orchestrating adaptive immune mechanisms and ultimately constrain inflammatory and immune responses (Park et al., 2003). IL-6 can use it for signal transduction (Kunzmann et al., 2010). After binding with its receptor gp130, the cell phosphorylates the JAK enzyme, activates downstream signal effect analysis STAT, and regulates related genes' expression into the nucleus. The activated JAKs could be further phosphorylated to transduce the intracellular signal and start STATs for activating NF- κ B (Tieying Hou, 2008). SOCS3 is one of the most active SOCS family members and the most critical inhibitor of JAK kinase and STAT signal transduction pathways (Porro et al., 2019). SOCS3 can also be strongly induced by IL-6 expression and STAT pathway activation was responsible for pro-inflammatory mediators in RAW264.7 cells (Lin et al., 2017). As demonstrated by the RNA-seq and western blot results (Fig. 8C), the higher expression levels of JAK2 and STAT3 with Al exposure was inhibited by ALA. Also, the SOCS3 protein expression was activated by ALA. These indicated that the blocking of STAT cascade is important for Al toxicity in macrophages.

MAPKs is a classic pathway that induces and promotes an inflammatory response. ERK1/2, p38, and JNK are essential members of this pathway (Guimaraes et al., 2013). Phosphory-

lation of p38 under inflammatory stimulation activates its downstream gene NF- κ B. The overproduction of inflammatory cytokines stimulating the MAPKs has been reported (Wang et al., 2020). In this current study, Al exposure elevated the phosphorylated expression of p38, ERK1/2, JNK, and p65 (Fig. 8A-B), suggesting the activation of those pathways and causing the cell apoptosis. It showed good association with KEGG analysis that MAPK pathway enriched in Al group (Supplementary Table 3). ALA treatment significantly repressed the protein phosphorylation level of p38, ERK1/2, JNK, and p65. Our findings agreed with some studies about Al toxicity inhibition, confirming that MAPK played crucial roles in ALA attenuated Al toxicity (Guo et al., 2016).

It is well known that HO-1 has special activities such as anti-inflammatory, antioxidant, and anti-apoptosis (Liu et al., 2016). Studies reported that anti-inflammatory effects could be achieved in the Nrf2 pathway and inducing the over-expression of HO-1 (Chung et al., 2008). Nrf2 mediates the expression of HO-1 to attenuate inflammation through the inhibition of NF- κ B translocation (Chung-Hsin et al., 2014; Kim et al., 2013). The results confirmed the mechanism that ALA induced HO-1 upregulated by Nrf2 to exert anti-inflammatory responses (Fig. 9A), involving in the secretion of pro-inflammatory mediators containing IL-6 and TNF- α (Fig. 9B). The results illustrated that HO-1 is contributing to the anti-inflammatory activity of ALA. Evidence indicated that HO-1 had been shown to inhibit inflammatory mediators' release by inhibiting STAT3 phosphorylation and NF- κ B p65 nuclear translocation (Liu et al., 2016). Based on the above pathways' critical role in signal transduction and cytokines transcription, we speculated that Al-induced toxicity might be inhibited by ALA through NF- κ B-STAT-HO-1 dependent mechanisms.

5. Conclusion

The current study assessed the ameliorative effects of ALA against Al-induced developmental toxicity in RAW264.7 cells. We constructed transcriptome profiles to reveal the differentially expressed genes in Al exposure and ALA treatment. We found that the genes enriched signaling pathways of TNF, NF- κ B, JAK/STAT, and MAPKs were involved in Al exposure-induced toxicity and the protective effects of ALA. Western blot analysis demonstrated that ALA inhibited Al-exerted toxicity and inflammatory response through STAT3 dependent NF- κ B pathway and HO-1 activation mediated by Nrf2. This study supports a new sight in Al-induced immunotoxicity's molecular mechanisms and the protective effects of ALA against Al toxicity.

Declaration of Competing Interest

The authors declare that they have no known competing financial interests or personal relationships that could have appeared to influence the work reported in this paper.

Acknowledgments

This work was supported by the National Natural Science Foundation of China (U21A20274, 31972041), Nature Science Foundation of Hubei Province (2019CFB583), the Agricultural Science and Technology Innovation Project of Chinese Academy of Agricultural Sciences (CAAS-ASTIP-2021-OCRI), the Earmarked Fund for China Agriculture Research

System (CARS-12), National Key R&D Program of China (2016YFD0401401), the Key Scientific Research Projects of Hubei Province (2020BCA086), the Achievement Transformation Project of Wuhan (2019030703011505).

Appendix A. Supplementary material

Supplementary data to this article can be found online at <https://doi.org/10.1016/j.arabjc.2023.104931>.

References

- Abulfadl, Y.S., El-Maraghy, N.N., Ahmed, A.E., Nofal, S., Badary, O.A., 2018. Thymoquinone alleviates the experimentally induced Alzheimer's disease inflammation by modulation of TLRs signaling. *Hum. Exp. Toxicol.* 37, 1092–1104.
- Ayuob, N.N., 2013. Can vitamin E and selenium alleviate the immunologic impact of aluminium on pregnant rats' spleens? *Cell. Immunol.* 284, 104–110.
- Bakour, M., Al-Waili, N.S., Menyiy, N.E., Imtara, H., Figuira, A., Al-Waili, T., Lyoussi, B., 2017. Antioxidant activity and protective effect of bee bread (honey and pollen) in aluminum-induced anemia, elevation of inflammatory makers and hepato-renal toxicity. *J. Food Sci. Technol.* 54, 4205–4212.
- Borai, I.H., Ezz, M.K., Rizk, M.Z., Aly, H.F., Fouad, G.I., 2017. Therapeutic impact of grape leaves polyphenols on certain biochemical and neurological markers in AlCl₃-induced Alzheimer's disease. *Biomed. Pharmacother.* 93, 837–851.
- Chen, Y., Chen, Y., Shi, C., Huang, Z., Zhang, Y., Li, S., Li, Y., Ye, J., Yu, C., Li, Z., 2018. SOAPnuke: a MapReduce acceleration-supported software for integrated quality control and preprocessing of high-throughput sequencing data. *Gigascience* 7, 1–6.
- Chen, J., Yang, S., Huang, S., Yan, R., Li, P., 2020. Transcriptome study reveals apoptosis of porcine kidney cells induced by fumonisin B1 via TNF signalling pathway. *Food Chem. Toxicol.* 139, 111274.
- Cheng, D., Zhang, X., Tang, J., Kong, Y., Wang, X., Wang, S., 2019. Chlorogenic acid protects against aluminum toxicity via MAPK/Akt signaling pathway in murine RAW264.7 macrophages. *J. Inorg. Biochem.* 190, 113–120.
- Chou, S.T., Lin, T.H., Peng, H.Y., Chao, W.W., 2019. Phytochemical profile of hot water extract of *Glechoma hederacea* and its antioxidant, and anti-inflammatory activities. *Life Sci.* 231, 116519.
- Chung, S.W., Liu, X., Macias, A.A., Baron, R.M., Perrella, M.A., 2008. Heme oxygenase-1-derived carbon monoxide enhances the host defense response to microbial sepsis in mice. *J. Clin. Invest.* 118, 239–247.
- Deng, G.F., Ke, L., Jing, M., Liu, F., Dai, J.J., Li, H.B., 2011. Aluminium content of some processed foods, raw materials and food additives in China by inductively coupled plasma-mass spectrometry. *Food Addit. Contam., Part B* 4, 248–253.
- Dimitrios, T., 2017. Assessment of lipid peroxidation by measuring malondialdehyde (MDA) and relatives in biological samples: analytical and biological challenges. *Anal. Biochem.* 524, 13–30.
- Dobin, A., Davis, C.A., Schlesinger, F., Drenkow, J., Zaleski, C., Jha, S., Batut, P., Chaisson, M., Gingeras, T.R., 2012. STAR: ultrafast universal RNA-seq aligner. *Bioinformatics* 29, 15–21.
- Dong, N., Li, X., Xue, C., Zhang, L., Wang, C., Xu, X., Shan, A., 2020. Astragalus polysaccharides alleviates LPS-induced inflammation via the NF- κ B/MAPK signaling pathway. *J. Cell. Physiol.* 235, 5525–5540.
- Farooq, M.A., Niazi, A.K., Akhtar, J., Ullah, S., Rengel, Z., 2019. Acquiring control: The evolution of ROS-Induced oxidative stress and redox signaling pathways in plant stress responses. *Plant Physiol. Biochem.* 141, 353–369.

- Gao, X., Chang, S., Liu, S., Peng, L., Sheng, J., 2020. Correlations between α -Linolenic Acid-Improved Multitissue Homeostasis and Gut Microbiota in Mice Fed a High-Fat Diet. *mSystems* 5, 000391-20.
- Guimaraes, M.R., Leite, F.R., Spolidorio, L.C., Kirkwood, K.L., Rossa, C., 2013. Curcumin abrogates LPS-induced pro-inflammatory cytokines in RAW 264.7 macrophages. evidence for novel mechanisms involving SOCS-1, -3 and p38 MAPK. *Arch. Oral Biol.* 58, 1309–1317.
- Guo, C., Yang, L., Wan, C.X., Xia, Y.Z., Zhang, C., Chen, M.H., Wang, Z.D., Li, Z.R., Li, X.M., Geng, Y.D., 2016. Anti-neuroinflammatory effect of Sophoraflavanone G from Sophora alopecuroides in LPS-activated BV2 microglia by MAPK, JAK/STAT and Nrf2/HO-1 signaling pathways. *Phytomedicine* 23, 1629–1637.
- Han, J.C., Mi, R.S., Lee, Y.M., Kim, J., Kim, J.K., Sang, G.K., Park, Yoon, J.H., 2008. 3,3'-Diindolylmethane Suppresses the Inflammatory Response to Lipopolysaccharide in Murine Macrophages. *J. Nutr.* 138, 17-23
- Han, L., Xia, X., Deng, Q., Zheng, C., Zhang, Z., Ji, Q., Xiang, X., 2019. Canolol induces apoptosis in human gastric carcinoma cell through PI3K/Akt signaling pathway. *Oil Crop Sci.* 4, 244–253.
- Hofseth, L.J., Ying, L., 2006. Identifying and defusing weapons of mass inflammation in carcinogenesis. *Biochim. Biophys. Acta Rev. Cancer* 1765, 74–84.
- Hu, C., Jing, L., Zhu, Y., Hao, S., Zhao, H., Bing, S., Li, Y., 2011. Effects of aluminum exposure on the adherence, chemotaxis, and phagocytosis capacity of peritoneal macrophages in rats. *Biol. Trace Elem. Res.* 144, 1032–1038.
- Jie, Ren, Eun, Jung, HanSung, Hyun, Chung, 2007. In Vivo and In Vitro anti-inflammatory activities of α -linolenic acid isolated from actinidia polygama fruits. *Arch. Pharmacol Res.* 30, 708-714
- Kim, S.W., Lee, H.K., Shin, J.H., Lee, J.K., 2013. Up-down regulation of HO-1 and iNOS gene expressions by ethyl pyruvate via recruiting p300 to Nrf2 and depriving It from p65. *Free Radic. Biol. Med.* 65, 468–476.
- Kim, K.B., Nam, Y.A., Kim, H.S., Hayes, A.W., Lee, B.M., 2014. α -Linolenic acid: nutraceutical, pharmacological and toxicological evaluation. *Food Chem. Toxicol.* 70, 163–178.
- Kunzmann, S., Ladenburger, A., Seehase, M., Thomas, W., Speer, C. P., 2010. Glucocorticoids potentiate IL-6-induced SP-B expression in H441 cells by enhancing the JAK-STAT signaling pathway. *Am. J. Physiol.: Lung Cell. Mol. Physiol.* 299, 578–584.
- Li, X., Fan, J., Luo, S., Yin, L., Liao, H., Cui, X., He, J., Zeng, Y., Qu, J., Bu, Z., 2021. Comparative transcriptome analysis identified important genes and regulatory pathways for flower color variation in *Paphiopedilum hirsutissimum*. *BMC Plant Biol.* 21, 495.
- Lin, H.W., Liu, C.W., Yang, D.J., Chen, C.C., Chen, S.Y., Tseng, J. K., Chang, T.J., Chang, Y.Y., 2017. *Dunaliella salina* alga extract inhibits the production of interleukin-6, nitric oxide, and reactive oxygen species by regulating nuclear factor- κ B/Janus kinase/signal transducer and activator of transcription in virus-infected RAW264.7 cells. *J. Food Drug Anal.* 25, 908–918.
- Liu, M., Fang, G., Yin, S., Zhao, X., Liu, Z., 2019. Caffeic acid prevented LPS-induced injury of primary bovine mammary epithelial cells through inhibiting NF- κ B and MAPK activation. *Mediat. Inflamm.* 2019, 1–12.
- Liu, H.H., Han, L., Xia, X.Y., Xiang, X., 2022. α -Linolenic acid alleviates aluminium chloride-induced toxicity in PC12 cells by activation of PKA-CREB-BDNF signaling pathway. *Oil Crop Science* 7 (2), 63–70.
- Liu, C.W., Lin, H.W., Yang, D.J., Chen, S.Y., Tseng, J.K., Chang, T.J., Chang, Y.Y., 2016. Luteolin inhibits viral-induced inflammatory response in RAW264.7 cells via suppression of STAT1/3 dependent NF- κ B and activation of HO-1. *Free Radical Biol. Med.* 95, 180–189.
- Love, M.I., Huber, W., Anders, S., 2014. Moderated estimation of fold change and dispersion for RNA-seq data with DESeq2. *Genome Biol.* 15, 550.
- Newairy, A.S.A., Salama, A.F., Hussien, H.M., Yousef, M.I., 2009. Propolis alleviates aluminium-induced lipid peroxidation and biochemical parameters in male rats. *Food Chem. Toxicol.* 47, 1093–1098.
- Park, E.J., Park, S.Y., Joe, E.H., Jou, I., 2003. 15d-PGJ2 and Rosiglitazone suppress Janus Kinase-STAT inflammatory signaling through induction of suppressor of Cytokine signaling 1 (SOCS1) and SOCS3 in Glia. *J. Biol. Chem.* 278, 14747–14752.
- Porro, C., Cianciulli, A., Trotta, T., Lofrumento, D.D., Panaro, M.A., 2019. Curcumin regulates anti-inflammatory responses by JAK/STAT/SOCS signaling pathway in BV-2 microglial cells. *Biology* 8, 51.
- Ren, J., Chung, S.H., 2007. Anti-inflammatory effect of alpha-linolenic acid and its mode of action through the inhibition of nitric oxide production and inducible nitric oxide synthase gene expression via NF- κ B and mitogen-activated protein kinase pathways. *J. Agric. Food Chem.* 55, 5073–5080.
- Tieying Hou, B.C.T., Ray, S., Adrian Recinos, I.I.I., Cui, R., Tilton, R.G., Brasier, A.R., 2008. Roles of IL-6-gp130 Signaling in Vascular Inflammation. *Curr. Cardiol. Rev.* 4, 179–192.
- Wang X, F.X., Yuan S, Jiao W, Liu B, Cao J, et al., 2017. Chlorogenic acid protects against aluminium-induced cytotoxicity through chelation and antioxidant actions in primary hippocampal neuronal cells. *Food Funct.* 8, 2924-2934
- Wang, H., Shao, B., Yu, H., Xu, F., Wang, P., Yu, K., Han, Y., Song, M., Li, Y., Cao, Z., 2018. Neuroprotective role of hyperforin on aluminum maltolate-induced oxidative damage and apoptosis in PC12 cells and SH-SY5Y cells. *Chem-Biol Interact.* 299, 15–26.
- Wang, X., Yu, N., Wang, Z., Qiu, T., Jiang, L., Zhu, X., Sun, Y., Xiong, H., 2020. *Akebia trifoliata* pericarp extract ameliorates inflammation through NF- κ B/MAPK signaling pathways and modifies gut microbiota. *Food Funct.* 11, 4682–4696.
- Weidenhamer, Jeffrey, D., Hudson, Michael, R., Kobunski, Peter, A., Gottesfeld, 2017. Metal exposures from aluminum cookware: An unrecognized public health risk in developing countries. *Sci. Total Environ.* 579, 805-813
- Wen, J., Khan, I., Li, A., Chen, X., Yang, P., Song, P., Jing, Y., Wei, J., Che, T., Zhang, C., 2019. Alpha-linolenic acid given as an anti-inflammatory agent in a mouse model of colonic inflammation. *Food Sci. Nutr.* 7, 3873–3882.
- Weng, M.H., Chen, S.Y., Li, Z.Y., Yen, G.C., 2020. Camellia oil alleviates the progression of Alzheimer's disease in aluminum chloride-treated rats. *Free Radic. Biol. Med.* 152, 411–421.
- Yao, Y.D., Shen, X.Y., Machado, J., Luo, J.F., Zhou, H., 2019. Nardochinoid B inhibited the activation of RAW264.7 macrophages stimulated by lipopolysaccharide through activating the Nrf2/HO-1 pathway. *Molecules* 24, 2482.
- Ye, S., Zheng, Q., Zhou, Y., Bai, B., Zhao, Z., 2019. Chlojaponilactone B attenuates lipopolysaccharide-induced inflammatory responses by suppressing TLR4-mediated ROS generation and NF- κ B signaling pathway. *Molecules* 24, 3731.
- Yeh, C.H., Yang, J.J., Yang, M.L., Li, Y.C., Kuan, Y.H., 2014. Rutin decreases lipopolysaccharide-induced acute lung injury via inhibition of oxidative stress and the MAPK–NF- κ B pathway. *ScienceDirect. Free Radical Biol. Med.* 69, 249–257.
- Zhang, H., Wang, P., Yu, H., Yu, K., Cao, Z., Xu, F., Yang, X., Song, M., Li, Y., 2018. Aluminum trichloride-induced hippocampal inflammatory lesions are associated with IL-1 β -activated IL-1 signaling pathway in developing rats. *Chemosphere* 203, 170.
- Zhang, H., Wei, M., Lu, X., Sun, Q., Wang, C., Zhang, J., Fan, H., 2020a. Aluminum trichloride caused hippocampal neural cells death and subsequent depression-like behavior in rats via the activation of IL-1 β /JNK signaling pathway. *Sci. Total Environ.* 715, 136942.
- Zhang, Y., Zhang, P., Yu, P., Shang, X., Li, Y., 2020b. Transcriptome analysis reveals the mechanism of common carp brain injury after exposure to lead. *Sci. Total Environ.* 743, 140796.